# Out-of-plane metal coordination for a true solvent-free molecular *lego building*: dodging the surface ligand effect for on-surface vacuum self-assembly

*Alessio Orbelli Biroli[1,2±], Alberto Calloni[3±], Alberto Bossi[1]*, Maddan. S. Jagadeesh[3†], Guglielmo Albani,[3] Lamberto Duò[3], Franco Ciccacci[3], Andrea Goldoni[4], Alberto Verdini,[5] Luca Schio,[5] Luca Floreano[5], Gianlorenzo Bussetti[1,3]**

Dr. A. Orbelli Biroli, Dr. A. Bossi, Prof. G. Bussetti,
Istituto di Scienze e Tecnologie Chimiche "G. Natta" del Consiglio Nazionale delle Ricerche (CNR-SCITEC), via Golgi 19, I-20133 Milano; PST via G. Fantoli 16/15, I-20138 Milano, Italy; and SmartMatLab Centre, via Golgi 19, I-20133 Milano, Italy.
E-mail: alberto.bossi@cnr.it
Dr. A. Orbelli Biroli,
Dipartimento di Chimica, Università di Pavia, via Taramelli 12, 27100 Pavia, Italy.
Dr. A. Calloni, Dr. M.S. Jagadeesh, Dr. G. Albani, Prof. L Duò, Prof. F. Ciccacci,
Department of Physics, Politecnico di Milano, p.za Leonardo da Vinci 32, I-20133 Milano, Italy. E-mail: gianlorenzo.bussetti@polimi.it
Dr. A. Goldoni,
Elettra Sincrotrone Trieste, s.s. 14 km 163.5 in Area Science Park, 34149 Trieste, Italy.
Dr. A. Verdini, Dr, L. Schio, Dr. L. Floreano,
Istituto Officina dei Materiali – CNR-IOM, Laboratorio TASC s.s. 14 km 163.5, 34149 Trieste, Italy.
± AOB and AC have contributed equally to this work.
† Current address: Department of Physics, Università degli Studi di Roma "La Sapienza", p.za A. Moro 5, I-00185 Roma, Italy.

Keywords: ideal contact interfaces; in vacuum 3D self-assembly; surface ligand effects; epitaxial growths; NEXAFS

ABSTRACT: The desirable self-assembly (SA) of repeated 2D stacked layers requires a "holistic analysis" of three interconnected components that are the electrode, the interface, and the molecular component; among them, the contact interface bears the largest burden of responsibilities. Epitaxial growth (EG) of coherent 2D+n stacked heterojunction by solvent-free deposition holds great promise despite the feasibility has never been demonstrated given multiple drawbacks (e.g., surface-ligand effect, SLE). Here, we demonstrate how a coherent 2D+n (n = 3) layered heterorganic film was grown on an archetypal Fe metal electrode. The groundbreaking achievement is the result of the in-vacuum integration of: (i) chemical decoupling of the basal organic layer (a ZnII-tetraphenylporphyrine, ZnTPP) from the metal

electrode, (ii) 2D-ordering of the ZnTPP commensurate to the substrate, (iii) rigid, stoichiometric and orthogonally arranged, molecule-to-molecule coupling between ZnTPP and a ditopic linear bridging ligand (i.e. DPNDI) guided by SA coordination chemistry, and (iv) sharp (chemical) termination of the layered film.

## 1. Introduction

Full control of the "bottom-up approach" is the ultimate goal in the miniaturization, at the atomic-scale, of ordered structures displaying specific functional properties relevant for nanotechnology and electronics miniaturization.[1] Self-assembling (SA) process (of atoms and molecules)[2] represents the most prominent way. SA nanomaterials are tailored on rationally designed molecular building blocks. The components interact via either spatially extended interactions, like van der Waals forces[3] and π-π coupling,[4] or directional interactions of different strength, like hydrogen bonding or covalent bonds, including metal coordination.[5] SA, *a priori*, enables to determine the stoichiometric ratio between the components as well as the geometric pattern of their arrangement. In the typical SA process the interacting building blocks are in solution and the solvent plays an important role favoring the intimate contact between the molecular components. Self-assembly (SA), with interacting building blocks in solution, has been verified in many electronic devices, [6–11] although the solvent limits many nanofabrications to single monolayer. Realizing weak or strong intermolecular attracting interactions, a sequence of equilibrium stages guides the system to the most stable structure thorough a trial-and-error approach. In this regard, coordination chemistry offers to SA the broadest range of degrees of freedom for the arrangement of a large variety of molecular architectures and, in solution, this has been plainly demonstrated.[12] Conversely, solvent-less SA is practically unexplored. In fact, a recent study just appeared in literature,[13] while the present work was in the submission stage. Nonetheless, the low temperature construction therein reported still requires the use of a

molecular precursor in order to join the building blocks, whereas we succeed in obtaining a molecule-molecule bonding, at room temperature, via a direct *lego* building process.

The perspective of technological applications of SA processes (for electronic, spintronic, biology, etc) has been investigated on the surface of different substrates, obtaining well-defined and "in-plane" 2D-supramolecular structures,[14–17] even in solvent-free environment by in-vacuum evaporation on surface.[18] Conversely, more sophisticate and versatile "out-of-plane" SA 3D-structures are still a "mirage" [19–23] and are currently obtained only with a properly "primed" functionalized surface (electrode) bearing a covalently linked (through anchoring groups, spacers, *etc.*) self-assembled monolayer (SAM); SAM may improve the electronic matching with an organic overlayer,[24] but does not allow to steer the molecular orientation of the growing film (or to go beyond a second 2D stacked layer of functionalized molecules).[25,26] This is a fundamental parameter to determine the transport properties of the organic film,[27] and to assure homogeneity of the molecule/electrode assembly.[28] Specific tilting angle of the primer with respect to the surface deviates the stepwise layer-by-layer growth direction away from the desired orthogonality, which would instead foster a more precise multilayer construction.[20,29–32] In addition, priming imposes many constrains to the chemical components and limits the assembly of this interface forcing for a more complex molecular design and engineering.[33]

An alternative strategy to obtain highly-oriented monolayer deposition, with orthogonal reciprocal assembly, involves the use of molecular template platforms with a specific geometrical feature able to steer and bind the second molecular unit by a covalent bond.[34,35] The weak epitaxial growth (WEG), by in-vacuum deposition, exploits the polarizability of extended organic molecules to achieve alternate stacking of single layers of molecules with complementary electronic affinity (e.g. donor/acceptor, like phthalocyanines and perylene derivatives).[9,36,37] This approach envisions the adsorption of molecules directly on the electrode surface,[38] without any chemical bond (physical contact). [39] An ideal

molecule/electrode interface is a formidable challenge[19] due to one final drawback: the surface-ligand effect (SLE).[40] In fact, the substrate (electrode) surface always works as a special ligand interacting with any deposited molecules and altering, unpredictably, their chemical reactivity. The situation becomes even worse when planar molecules (first-choice for 2D scalable system) such as porphyrinic compounds,[40] are exploited in a device. Metalloporphyrins take advantage from the precise geometric control brought by the metal hybridization with the tetrapyrrolic pocket to define a specific coordination configuration, which may technically comply the geometric prerequisite and can be adopted as molecular platform when lying flat on a surface. However, the metal center prerogative can be chemically frustrated by the SLE thus destabilizing (due to *trans*-effect) further interactions with any new partner (i.e. a ligand) in the SA process.[41]

A first strategy proposed to minimize the SLE is to choose low-interacting surfaces, such as gold, graphite, insulating oxides or an organic crystal.[11] Unfortunately, this approach limits the research scope and precludes the use of far more interesting materials (*e.g.*, iron), which can drive special (*e.g.*, magnetic) couplings. Struggling with these difficulties, many researches focused their attention in describing the SLE in some interesting case-studies.[41]

A powerful method to observe the SLE is X-ray photoemission spectroscopy: a comparison among the spectral features (as due to the highest occupied molecular orbitals, HOMOs) of an organic thin film (tens of nanometers thick) with those of a single layer can highlight either chemical changes produced by SLE or the appearance of new interaction-states in the spectra.[42] In this scenario, our recent evidence of the almost unperturbed HOMO levels of porphyrins (i.e. **ZnTPP**) grown on an iron-oxide single layer was quite surprising.[43] Such a substrate, known as Fe(001)-$p(1 \times 1)$O, is the outcome of a special strategy for surface passivation, where oxygen atoms stably fill the hollow-sites of the iron surface reducing the molecules/metal interaction, nonetheless preserving the transport properties and magnetic couplings.[44,45] The HOMO levels investigation, however, seems not a conclusive proof that

**ZnTPP** reactivity (localized on the $Zn^{II}$ ion) is really preserved (therefore dodging the SLE), being the HOMO levels distributed on the entire molecular π-skeleton.

In this paper we provide evidence that **ZnTPP** molecules (on oxygen-passivated iron surface)[43] fully maintain the penta-coordination of the $Zn^{II}$ metal ion by proving the binding ability of $Zn^{II}$ ion towards suitable compounds.[46,47] We further demonstrate a precise and stoichiometric layer-by-layer growth by vacuum thermal deposition of a 3D covalent organic framework driven by metal coordination as sketched in **Figure 1**.

## 2. Result and discussion

Starting from a highly ordered monolayer of **ZnTPP** on Fe(001)-*p*(1 × 1)O it was possible to deposit directly a second monolayer of a ditopic linear bridging ligand, in a stoichiometric amount, directly onto the axial free coordinative site of the metal with an atomic precision; the ditopic ligand is N,N'-di(4-pyridyl)-1,4,5,8-naphthalenetetracarboxdiimide (**DPNDI**), where the naphthalene diimide scaffold (see **Figure 1**) is functionalized at the N,N' positions with two pyridine groups.[32] DPNDI, with a simple synthesis, is readily available and can be straightforwardly loaded and processed inside the vacuum chamber.

This **DPNDI-ZnTTP** construct becomes the new template surface where the bridging ligand allows the perfect organization of a third layer of metalloporphyrin, e.g. **ZnTPP**, as a capping layer, or **CoTPP**, as a new starting layer for a further layer-by-layer deposition (see Figure 1 and S2 in SI for the whole multilayer structure cartoon).[48]

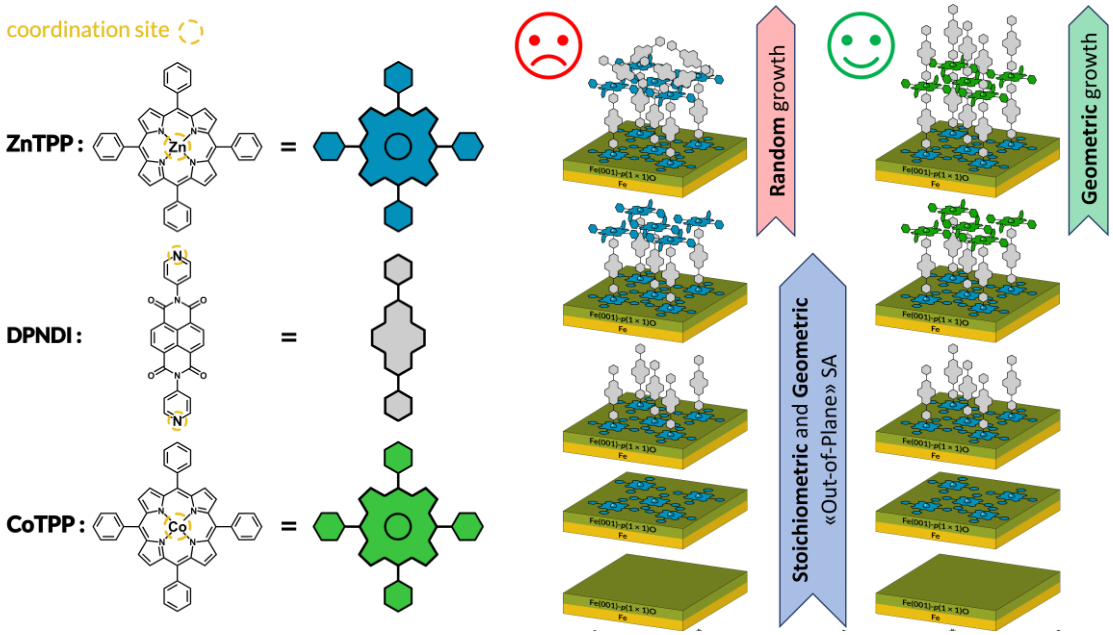


**Figure 1**. right, molecular structures of **ZnTPP** and **DPNDI** and **CoTPP** together with the schematics. The circles indicate the coordination sites for clarity; left, proposed molecular construction designed in this work.

The axial coordination site of the **ZnTPP** is available to bind the pyridine N atom of the DPNDI[47] if the Zn central atom (tetra-coordinated to the four in-plane porphyrin N atoms) is not perturbed by the buried substrate. From orbital symmetry considerations, coordinated **DPNDI** is expected to have an orientation normal to the plane of the porphyrin macrocycle (see **Figure 2** *a1* and *a2*). Conversely, SLE interaction between the $Zn^{II}$ ion and the substrate would preclude the **DPNDI-ZnTPP** assembly and its characteristic geometrical configuration.

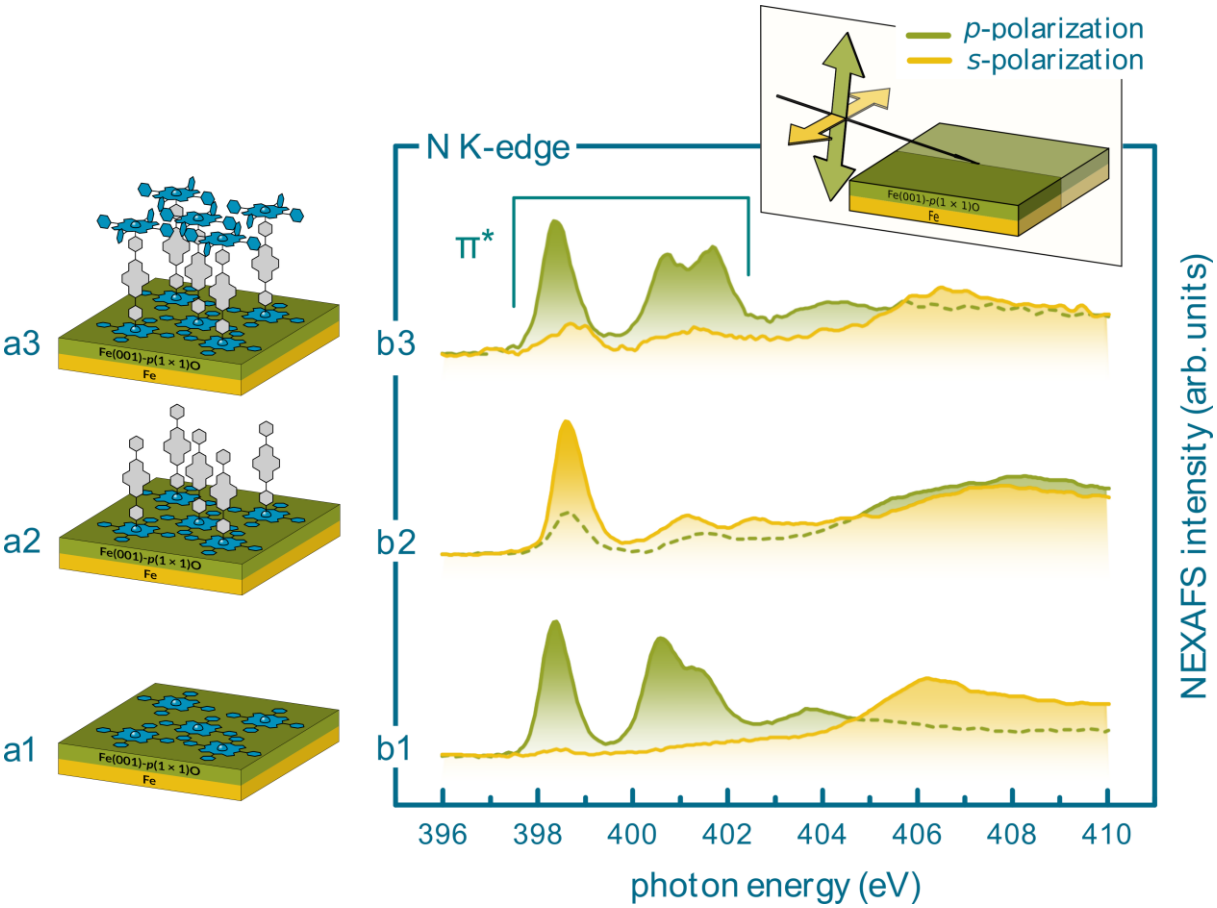


**Figure 2**. *a1-a3*: bottom-up architecture sketch; the arrangement shown is only possible when the first (*a1*) porphyrin layer is not perturbed by the substrate (SLE is dodged). *b1-b3*: NEXAFS spectra characterizing each construction *a1-a3* steps, only the contribution from the topmost layer is shown, retrieved by subtracting the (attenuated) signal from the underlying structure.[49] Our results give a direct evidence that the molecule/substrate orientations are in line with the expected sketched structure. The average molecular orientation can be determined from the intensity ratio of the π*-symmetry resonances at 398-402 eV, as measured in *s*- and *p*-polarization (see text for details).

Near Edge X-ray Absorption Fine Structure (NEXAFS) spectroscopy, performed at the N K-edge with both *p*- and *s*-polarized synchrotron light, is the exclusive technique that is able to disclose the average molecular orientation of both porphyrins and bridging ligands, since both molecules possess a π* symmetry lowest unoccupied molecular orbital (LUMO), which shows a dichroic response under the absorption of linearly polarized light. The NEXAFS intensity is at maximum when the polarized electric field is normal to the nodal plane of the π* orbital (of the tetrapyrrolic macrocycle or naphthalene diimide one) and drops to zero when the incident electric field is parallel to the nodal plane.

The NEXAFS spectra shown in **Figure 2**, *spectra b1*, display a strong dichroism of the π* resonances in *p*- and *s*-polarization, indicating a very homogeneous orientation of the **ZnTPP** layer, with the macrocycle parallel to the surface (*spectra b1*). This picture completely changes upon the deposition of **DPNDI** molecules (*spectra b2*). After the subtraction of the buried porphyrin film contribution, the NEXAFS spectrum in *s*-polarization results now dominated by the strong resonance of the π* LUMO of the DPNDI molecules. DPNDI molecules are thus oriented perpendicular to the substrate. This unequivocally implies that they are installed and coordinated to the $Zn^{II}$ ion of **ZnTPP** and are initiating an ordered "out-of-plane" growth. The **DPNDI-ZnTPP** construct proves that the $Zn^{II}$ ion core of **ZnTPP** maintains the axial-coordinative site available for bonding, thus the passivation by oxidation of the topmost Fe layer allowed us to effectively "dodge" the SLE.

Having pyridine groups at both sides, the **DPNDI** molecule can also act as a spacer (as currently prescribed in Ref. [19]) for the chemical organization of a second **ZnTPP** molecule far from the substrate (*sketch a3* in **Figure 2**). As a results, after sublimation of **ZnTPPs** onto the **DPNDI-ZnTPP** bilayer, the molecules of the uppermost layer are indeed found to lie flat and parallel to the buried substrate (*sketch a3*). In fact, π*-symmetry resonances rise again in *p*-polarization NEXAFS (*spectra b3*) that, after the subtraction of the **DPNDI** contribution, closely mimic the π* contribution of the first layer **ZnTPP** spectra b1.

At this engineering construction step, on-surface coordination chemistry (pyridine-$Zn^{II}$ ion link) emerges as a straightforward and powerful tool for a neat and controlled step-by-step molecular bottom-up self-assembly. Nonetheless, this assembly process cannot be further repeated on the uppermost porphyrin molecules. In fact, the top **ZnTPPs** of *sketch a3* are coordinated to the underneath **DPNDI** molecules (spacers), hence the $Zn^{II}$ ion is no longer available for further controlled depositions. This picture is verified by NEXAFS analysis after a new sublimation of **DPNDI** molecules on the sample. The negligible linear dichroism (**Figure 3**, *spectra b4* with respect to *spectra b2*) proves that **DPNDI** molecules of the

tompost layer are randomly oriented on the ZnTPP (capping) layer underneath due to the lack of any available coordination site.

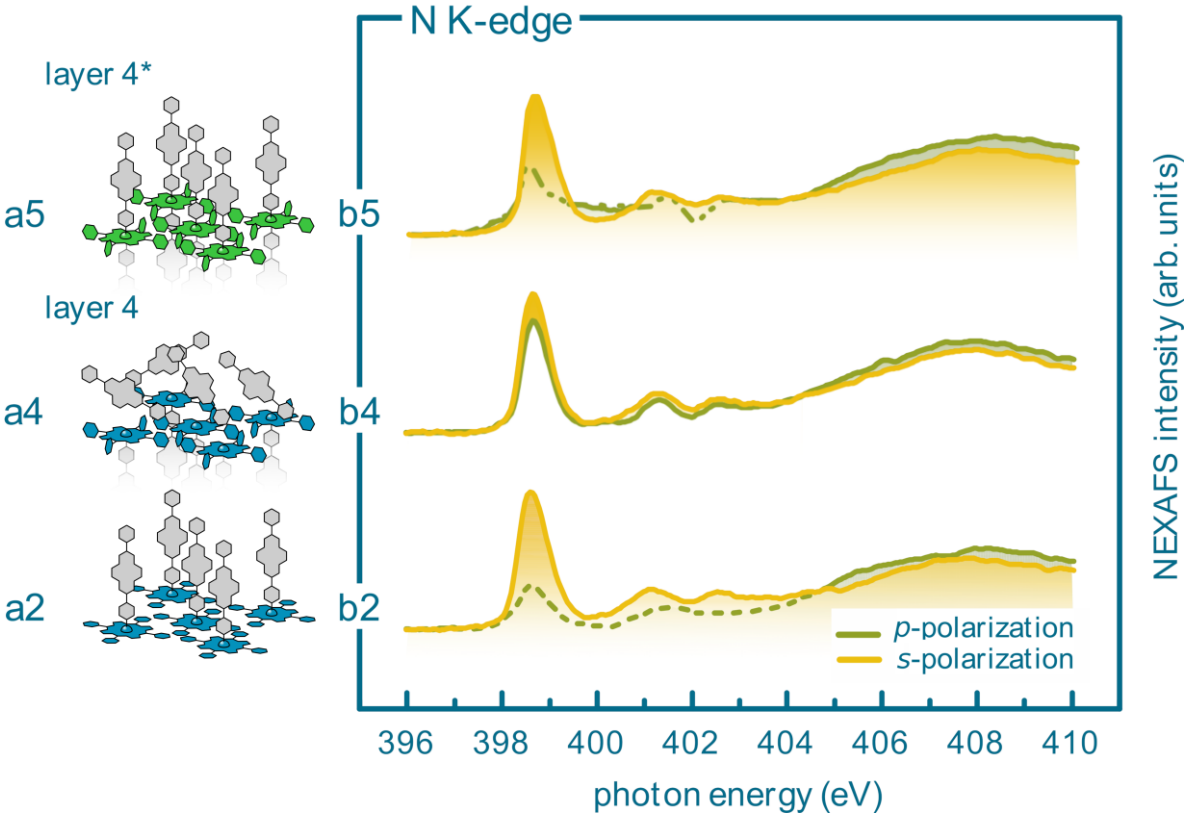


**Figure 3**. *a2*, *a4*: bottom-up architecture sketches evidencing the geometric orthogonal growth of **DPNDI** on "active" **ZnTPP** in contrast to its random orientation once grown on top of a "inert" **ZnTPP** layer, whose $Zn^{II}$ ion coordination site has been saturated by the underneath layer of **DPNDI** (as in layer *a3*, Fig.2); NEXAFS spectra (analyzed following the procedure described in the caption of Figure 2) evidence perpendicular arrangement of **DPNDI** molecules *b2*, while the equivalence of *p*- and *s*- polarization spectra characterize a random distribution in *b4*. *a5*: bottom-up architecture sketch of the geometric orthogonal growth of **DPNDI** on top of **CoTPP** (previously grown on **DPNDI**) which still has an available coordination site.

In an attempt to grow an additional ordered layer of molecules coordinated to the metal center, a different metal porphyrin, i.e. **CoTPP**, was used in the construction of the layer 3 instead of **ZnTPP**. **CoTPP** grown over the **DPNDI-ZnTPP** bilayer assemble with a geometry equivalent to the that of **ZnTPP** and the NEXAFS dichroism analysis indicates the **CoTPP** macrocycle to be oriented parallel to the buried substrate. Differently from the $Zn^{II}$ ion, the $Co^{II}$ one has two axial coordination sites: one of them is used for the **CoTPP** coordination to

the buried **DPNDI** of layer 2, the second one is still free to coordinate another **DPNDI** molecule in layer 4 (labeled as layer 4* in *sketch a5*). Strikingly, the NEXAFS spectra show a clear linear dichroism (*spectra b5*) that confirms the expected vertical geometry assembly of the topmost DPNDI layer. An important aspect of this vertical construction is the coherent translation to the topmost layer of the in-plane spatial distribution of the first layer. In fact, the pristine (5 × 5) commensurate and long range ordered symmetry of ZnTPP in the contact layer is not perturbed by the growth of DPNDI on top of it and further porphyrin layer, as observed by reflection high-energy electron diffraction patterns (see Fig. S3 in SI).

**3. Conclusion.**

We proved a state-of-the-art strategy for the assembly of single-molecule/electrode interface based on an architecture without any chemically bonded spacer. All the known limits deriving from the facts that i) a surface can act as a ligand, and ii) the interaction between molecules and surface is practically a special type of chemical bonding, have been sidestepped. Such a situation drove our research in the realization by self-assembly of "out-of-plane" covalently bond 3D-structures with precise stoichiometry and geometry control. We remark that passivation by surface oxidation may apply to alternative metals (Cu, Co, Ni, Al), according to the required applications, where different porphyrin assembly may result (not necessarily displaying long range order), but with the orientation of the macrocycle always parallel to the substrate,[40] thus exposing towards vacuum the axial coordination site at the metal center. With this contribution, we propose a physical molecule/electrode contact as a first strategy for dodging the SLE. We proved that an ideal molecule-electrode interface can be obtained, where the molecular coordination sites of the first organic monolayer are preserved from any interaction with the surface. Our approach demonstrates the possible exploitation in true bottom-up device engineering of molecular 3D coherent growth by vapour phase deposition through coordination chemistry. As a result of our *Lego* construction, the topmost molecule is

directly coupled to the substrate via metal coordination of the pyridyl groups, which offers an ultra-fast charge transfer channel (femtosec timescale), alternative to the intermolecular hopping mechanism that, however fast, yields charge transfer rates slower by orders of magnitude.

**4. Methods.**

The Fe(001)-*p*(1 × 1)O substrate was prepared according to the protocol reported in literature.[42,50] The clean iron substrate is exposed to few langmuir of molecular oxygen (grade 5.5) and then annealed at about 970 K. Porphyrins, provided by Sigma Aldrich (purity of 99.8%) and used without any further purification, were evaporated from a Knudsen crucible at about 570 K. The growth chamber is equipped with a quartz microbalance able to measure few parts of a ML per minute, where the surface coverage was preliminarily calibrated as 1 ML = 3.06 Å.[42]

N,N'-di(4-pyridyl)-1,4,5,8-naphthalenetetracarboxdiimide (DPNDI) was synthesized according to a previously published procedure.[51] The compound was further purified by train sublimation prior to the use.

The molecule sublimation does not break or alter either porphyrin or DPNDI, as evidenced by the stoichiometry analysis. In **Figure 4**, XPS spectra of the main molecular elements are reported.

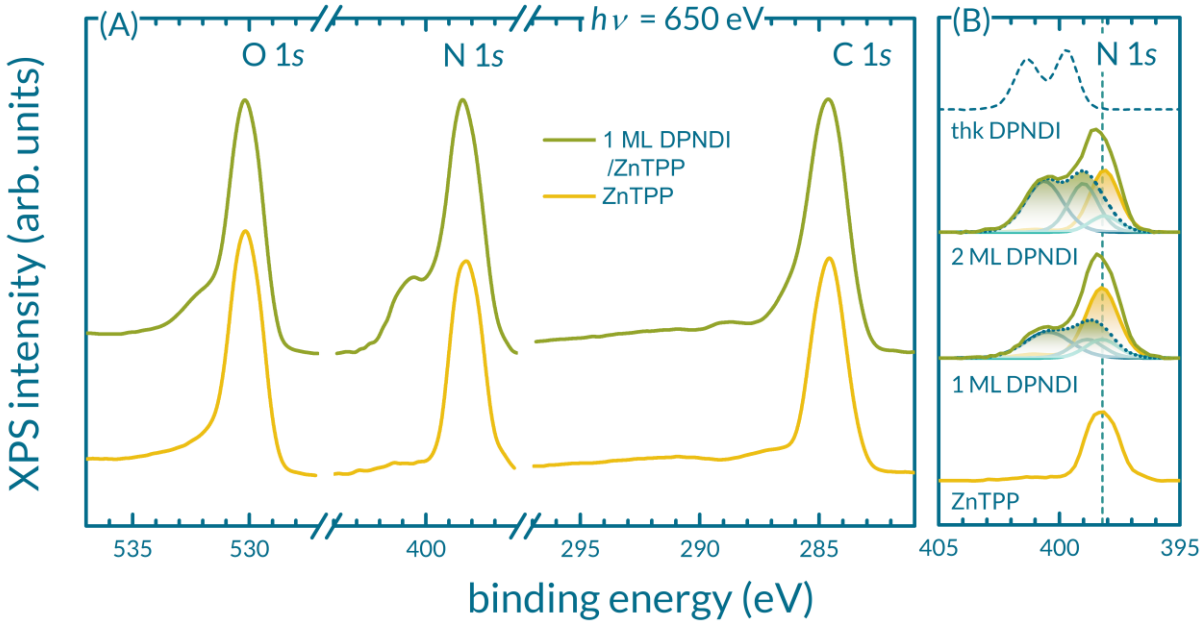


**Figure 4**. (A) XPS spectra of the main molecular elements. (B) Stoichiometry analysis of the deposited DPNDI (ML: monolayer; thk: thick, bulk layer). The spectra are to scale, but rigidly shifted by a vertical offset for a better visual comparison. [52]

The oxygen (see panel A) observed on the layer 1 (ZnTPP) is due to the buried passivated iron substrate. A shoulder at higher binding energy (BE) appears when DPNDI molecules are deposited on the sample. This contribution is related to the four oxygen atoms that characterize the naphthalene diimide scaffold (see molecular structure in **Figure 1**). Nitrogen analysis is more complex due to the presence of N element on both DPNDI and porphyrin molecules. The latter is characterized by a single feature, as reported in panel (B). The DPNDI system counts 4 N atoms having different bounds: 2 N atoms are placed in the naphthalene diimide scaffold, while the other 2 belong to the pyridine groups. Our data confirm the 1:1 ratio between these features [green shadow area in panel (B)]. Finally, to assess a chemical bond between the DPNDI and the buried ZnTPP film, we have to compare the N 1*s* feature before and after a thermal treatment of the sample. In **Figure 5**, we observe that if a double amount of DPNDI is originally deposited on the ZnTPP layer 1 and then the sample is annealed at a temperature below 200 °C, the N 1*s* spectrum is superimposable to the one formerly collected on the 1:1 DPNDI-ZnTPP system (labeled as 1 ML in the figure). This

fact indicates that molecules in excess of the available zinc coordination sites simply desorb upon annealing, thus proving the direct bonding of the remaining DPNDI layer to the ZnTPP one.

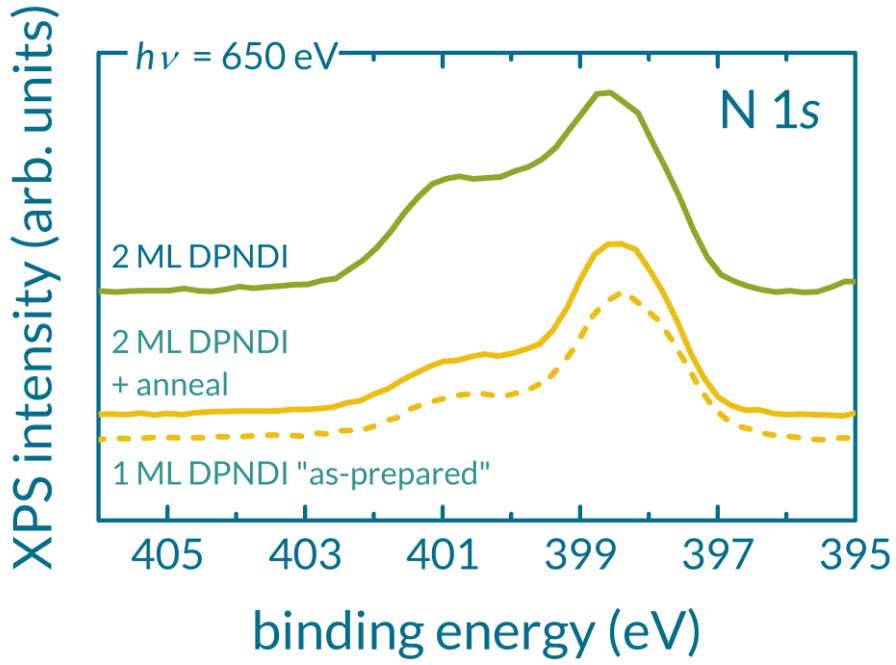


**Figure 5**. XPS spectra of N 1s collected before and after a thermal annealing of a 2 ML DPNDI film grown onto the ZnTPP layer 1. After the annealing, the spectrum is superimposable on that one collected on a 1 ML DPNDI film. The spectra are to scale, but rigidly shifted by a vertical offset for a better visual comparison.

NEXAFS spectra were acquired at the ALOISA beamline at the Elettra synchrotron radiation facility (Trieste, Italy) in partial electron yield mode by means of a channeltron equipped with a negatively biased grid to filter out low energy secondary electrons and increase the signal to background ratio. To investigate the sample dichroism, spectra have been collected with the surface oriented either parallel to the electric field (*s*-polarization) or closely normal to it (*p*-polarization), while the light grazing angle was kept constant at 6°. The photon energy resolution was set to 80 meV. The photon flux normalization and the energy calibration are described elsewhere.[53] The NEXAFS spectra of the first ZnTPP layer are simply normalized to the corresponding spectra measured on the Fe(001)-*p*(1 × 1)O surface before molecular deposition. All the spectra of each further step of deposition are shown after (weighted) subtraction of the corresponding spectra in the previous deposition step.

**Author contributions.**
A.O.B. and A.C.: conceptualization, data curation and analysis; M. S. J., G. A., A. V., A. G. and L. S.: investigation; L. F.: supervision, writing – review; A.B. and G. B. conceptualization, supervision, writing - review & editing; A. V., L. D. and F. C.: writing - review & editing, supervision.

**Competing interests.**
The authors declare no competing interest.

**Supporting Information**
Supporting Information is available from the Wiley Online Library or from the author.

**Acknowledgements**
((Acknowledgements, general annotations, funding. Other references to the title/authors can also appear here, such as "Author 1 and Author 2 contributed equally to this work."))

Received: ((will be filled in by the editorial staff))
Revised: ((will be filled in by the editorial staff))
Published online: ((will be filled in by the editorial staff))

References

[1] J. C. Love, L. A. Estroff, J. K. Kriebel, R. G. Nuzzo, G. M. Whitesides, *Self-assembled monolayers of thiolates on metals as a form of nanotechnology*, Vol. 105, **2005**.

[2] W. Lu, In *Encyclopedia of Nanotechnology* (Ed.: Bhushan, B.), Springer Netherlands, Dordrecht, **2012**, pp. 2371–2382.

[3] C. R. Martinez, B. L. Iverson, *Chem. Sci.* **2012**, *3*, 2191.

[4] S. Grimme, *Angew. Chemie - Int. Ed.* **2008**, *47*, 3430.

[5] T. Kudernac, S. Lei, J. A. A. W. Elemans, S. De Feyter, *Chem. Soc. Rev.* **2009**, *38*, 402.

[6] E. Lörtscher, B. Gotsmann, Y. Lee, L. Yu, C. Rettner, H. Riel, *ACS Nano* **2012**, *6*, 4931.

[7] P. Gehring, J. M. Thijssen, H. S. J. van der Zant, *Nat. Rev. Phys.* **2019**, *1*, 381.

[8] R. C. Vasconcelos, V. F. P. Aleixo, J. Del Nero, *Phys. E Low-Dimensional Syst.*

*Nanostructures* **2017**, *86*, 142.

[9] Y. S. Chen, M. Y. Hong, G. S. Huang, *Nat. Nanotechnol.* **2012**, *7*, 197.

[10] W. Auwärter, K. Seufert, F. Bischoff, D. Ecija, S. Vijayaraghavan, S. Joshi, F. Klappenberger, N. Samudrala, J. V. Barth, *Nat. Nanotechnol.* **2012**, *7*, 41.

[11] G. Bussetti, M. Campione, M. Riva, A. Picone, L. Raimondo, L. Ferraro, C. Hogan, M. Palummo, A. Brambilla, M. Finazzi, L. Duò, A. Sassella, F. Ciccacci, *Adv. Funct. Mater.* **2014**, *24*, 958.

[12] S. Datta, M. L. Saha, P. J. Stang, *Acc. Chem. Res.* **2018**, *51*, 2047.

[13] Z. Wang, K. Qian, M. A. Öner, P. S. Deimel, Y. Wang, S. Zhang, X. Zhang, V. Gupta, J. Li, H.-J. Gao, D. A. Duncan, J. V. Barth, X. Lin, F. Allegretti, S. Du, C.-A. Palma, *ACS Appl. Nano Mater.* **2020**, acsanm.0c02237.

[14] S. Stepanow, N. Lin, J. V. Barth, *J. Phys. Condens. Matter* **2008**, *20*.

[15] N. Miyashita, D. G. Kurth, *J. Mater. Chem.* **2008**, *18*, 2636.

[16] R. Madueno, M. T. Räisänen, C. Silien, M. Buck, *Nature* **2008**, *454*, 618.

[17] A. Ciesielski, C. A. Palma, M. Bonini, P. Samori, *Adv. Mater.* **2010**, *22*, 3506.

[18] N. Lin, A. Langner, S. L. Tait, C. Rajadurai, M. Ruben, K. Kern, *Chem. Commun.* **2007**, *1*, 4860.

[19] N. Xin, J. Guan, C. Zhou, X. Chen, C. Gu, Y. Li, M. A. Ratner, A. Nitzan, J. F. Stoddart, X. Guo, *Nat. Rev. Phys.* **2019**, *1*, 211.

[20] A. Facchetti, E. Annoni, L. Beverina, M. Morone, P. Zhu, T. J. Marks, G. A. Pagani, *Nat. Mater.* **2004**, *3*, 910.

[21] R. Cao, A. M. Díaz-García, R. Cao, *Coord. Chem. Rev.* **2009**, *253*, 1262.

[22] G. De Ruiter, M. Lahav, H. Keisar, M. E. Van Der Boom, *Angew. Chemie - Int. Ed.* **2013**, *52*, 704.

[23] R. Sakamoto, K. H. Wu, R. Matsuoka, H. Maeda, H. Nishihara, *Chem. Soc. Rev.* **2015**, *44*, 7698.

[24] W. Chen, X. Y. Gao, D. C. Qi, S. Chen, Z. K. Chen, A. T. S. Wee, *Adv. Funct. Mater.* **2007**, *17*, 1339.

[25] A. Cossaro, M. Puppin, D. Cvetko, G. Kladnik, A. Verdini, M. Coreno, M. De Simone, L. Floreano, A. Morgante, *J. Phys. Chem. Lett.* **2011**, *2*, 3124.

[26] Z. Jia, V. W. Lee, I. Kymissis, L. Floreano, A. Verdini, A. Cossaro, A. Morgante, *Phys. Rev. B - Condens. Matter Mater. Phys.* **2010**, *82*, 1.

[27] H. Sirringhaus, P. J. Brown, R. H. Friend, M. M. Nielsen, K. Bechgaard, B. M. W. Langeveld-Voss, A. J. H. Spiering, R. A. J. Janssen, E. W. Meijer, P. Herwig, D. M. de Leeuw, *Nature* **1999**, *401*, 685.

[28] A. Cossaro, D. Cvetko, L. Floreano, *Phys. Chem. Chem. Phys.* **2012**, *14*, 13154.

[29] M. Koepf, F. Chérioux, J. A. Wytko, J. Weiss, *Coord. Chem. Rev.* **2012**, *256*, 2872.

[30] B. H. Lee, B. Yoon, A. I. Abdulagatov, R. A. Hall, S. M. George, *Adv. Funct. Mater.* **2013**, *23*, 532.

[31] I. Stassen, D. De Vos, R. Ameloot, *Chem. - A Eur. J.* **2016**, *22*, 14452.

[32] J. L. Zhuang, A. Terfort, C. Wöll, *Coord. Chem. Rev.* **2016**, *307*, 391.

[33] M. K. Khan, P. R. Sundararajan, *J. Phys. Chem. B* **2013**, *117*, 5705.

[34] B. Baisch, D. Raffa, U. Jung, O. M. Magnussen, C. Nicolas, J. Lacour, J. Kubitschke, R. Herges, *J. Am. Chem. Soc.* **2009**, *131*, 442.

[35] F. L. Otte, S. Lemke, C. Schütt, N. R. Krekiehn, U. Jung, O. M. Magnussen, R. Herges, *J. Am. Chem. Soc.* **2014**, *136*, 11248.

[36] R. R. Lunt, J. B. Benziger, S. R. Forrest, *Adv. Mater.* **2007**, *19*, 4229.

[37] W. Chen, H. Huang, S. Chen, X. Y. Gao, A. T. S. Wee, *J. Phys. Chem. C* **2008**, *112*, 5036.

[38] Z. Lin, Y. Huang, X. Duan, *Nat. Electron.* **2019**, *2*, 378.

[39] H. Chen, W. Zhang, M. Li, G. He, X. Guo, *Chem. Rev.* **2020**, *120*, 2879.

[40] J. M. Gottfried, *Surf. Sci. Rep.* **2015**, *70*, 259.

[41] W. Hieringer, K. Flechtner, A. Kretschmann, K. Seufert, W. Auwärter, J. V. Barth, A. Görling, H. P. Steinrück, J. M. Gottfried, *J. Am. Chem. Soc.* **2011**, *133*, 6206.

[42] C. Castellarin Cudia, P. Vilmercati, R. Larciprete, C. Cepek, G. Zampieri, L. Sangaletti, S. Pagliara, A. Verdini, A. Cossaro, L. Floreano, A. Morgante, L. Petaccia, S. Lizzit, C. Battocchio, G. Polzonetti, A. Goldoni, *Surf. Sci.* **2006**, *600*, 4013.

[43] G. Bussetti, A. Calloni, M. Celeri, R. Yivlialin, M. Finazzi, F. Bottegoni, L. Duò, F. Ciccacci, *Appl. Surf. Sci.* **2016**, *390*, 856.

[44] A. Picone, M. Riva, A. Brambilla, A. Calloni, G. Bussetti, M. Finazzi, F. Ciccacci, L. Duò, **2016**, *71*, 32.

[45] M. S. Jagadeesh, A. Calloni, A. Brambilla, A. Picone, A. Lodesani, L. Duò, F. Ciccacci, M. Finazzi, G. Bussetti, *Appl. Phys. Lett.* **2019**, *115*.

[46] C. Trinh, M. T. Whited, A. Steiner, C. J. Tassone, M. F. Toney, M. E. Thompson, *Chem. Mater.* **2012**, *24*, 2583.

[47] S. Fukuzumi, T. Honda, K. Ohkubo, T. Kojima, *Dalt. Trans.* **2009**, 3869.

[48] When CoTPP is directly grown onto the Fe(001)-*p*(1 × 1)O, the organic superstructure is again 5 × 5 but rotated of about 37° with respect the main iron crystal directions. In addition, ZnTPP is able to create a continueous wetting layer while, CoTPP, is or, .

[49] T. Schiros, G. Kladnik, D. Prezzi, A. Ferretti, G. Olivieri, A. Cossaro, L. Floreano, A. Verdini, C. Schenck, M. Cox, A. A. Gorodetsky, K. Plunkett, D. Delongchamp, C. Nuckolls, A. Morgante, D. Cvetko, I. Kymissis, *Adv. Energy Mater.* **2013**, *3*.

[50] A. Summerfield, M. Baldoni, D. V. Kondratuk, H. L. Anderson, S. Whitelam, J. P. Garrahan, E. Besley, P. H. Beton, *Nat. Commun.* **2019**, *10*, 1.

[51] D. R. Trivedi, Y. Fujiki, Y. Goto, N. Fujita, S. Shinkai, K. Sada, *Chem. Lett.* **2008**, *37*, 550.

[52] V. Lanzilotto, G. Lovat, G. Fratesi, G. Bavdek, G. P. Brivio, L. Floreano, *J. Phys. Chem. Lett.* **2015**, *6*, 308.

[53] L. Floreano, A. Cossaro, R. Gotter, A. Verdini, G. Bavdek, F. Evangelista, A. Ruocco, A. Morgante, D. Cvetko, *J. Phys. Chem. C* **2008**, *112*, 10794.

Evidence for the construction of an out-of-plane (normal to the surface) self-assembled heterostructure guided by in-vacuum coordination chemistry. The whole construct**,** albeit ordered and commensurate, is settled on a pure "physical contact interface" ever realized between a molecule and a metallic surface.

A. Orbelli Biroli[1,2±], A. Calloni[3±], A. Bossi[1]*, M. S. Jagadeesh[3†], G. Albani,[3] L. Duò[3], F. Ciccacci[3], A. Goldoni[4], A. Verdini,[5] L. Schio,[5] L. Floreano[5], G. Bussetti[1,3]*

## Out-of-plane metal coordination for a true solvent-free molecular *lego building*: dodging the surface ligand effect for on-surface vacuum self-assembly

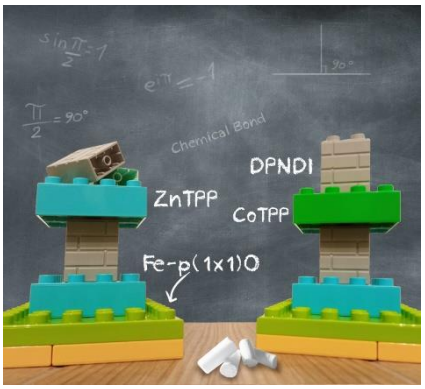

# Supporting Information

**Out-of-plane metal coordination for a true solvent-free molecular *lego building*: dodging the surface ligand effect for on-surface vacuum self-assembly**

*Alessio Orbelli Biroli[1,2±], Alberto Calloni[3±], Alberto Bossi[1]*, Maddan. S. Jagadeesh[3†], Guglielmo Albani,[3] Lamberto Duò[3], Franco Ciccacci[3], Andrea Goldoni[4], Alberto Verdini,[5] Luca Schio,[5] Luca Floreano[5], Gianlorenzo Bussetti[1,3]**

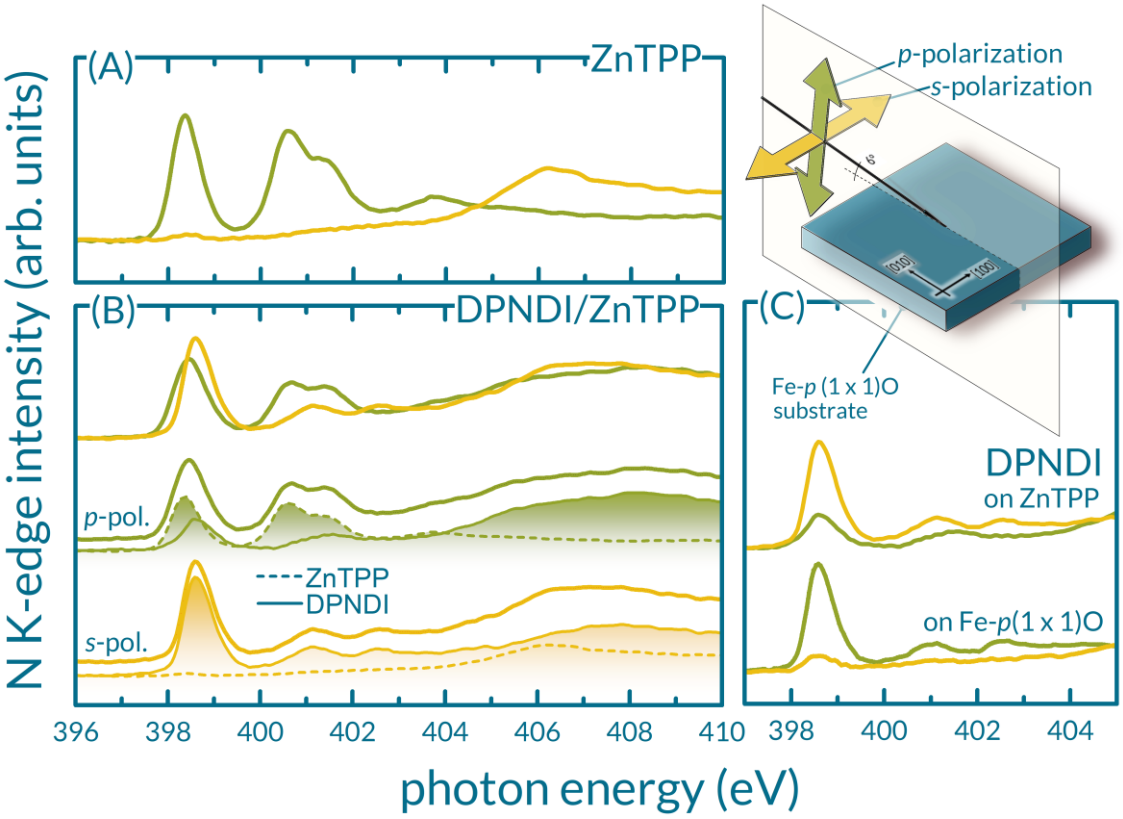


**Figure S1**. (A) NEXAFS spectra from the first ZnTPP layer, as reported in **Figure 2**, *spectra 1b*. The featureless NEXAFS contribution of the Fe-*p*(1 × 1)O substrate has been subtracted. (B) Top spectra: raw data acquired on the DPNDI/ZnTPP system. Lower spectra: subtraction of the signal from the buried ZnTPP layer (A) in view of enhancing the contribution of DPNDI molecules. The subtraction strategies are reported in the literature (*1*). (C) Comparison of the DPNDI growth on the ZnTPP first layer (upper spectra) and directly on Fe-*p*(1 × 1)O (lower spectra), where the molecules lie flat (enhancement of the *p*-polarization signal). The collected results prove the key role of the $Zn^{II}$ ion when ZnTPP molecules are not perturbed.

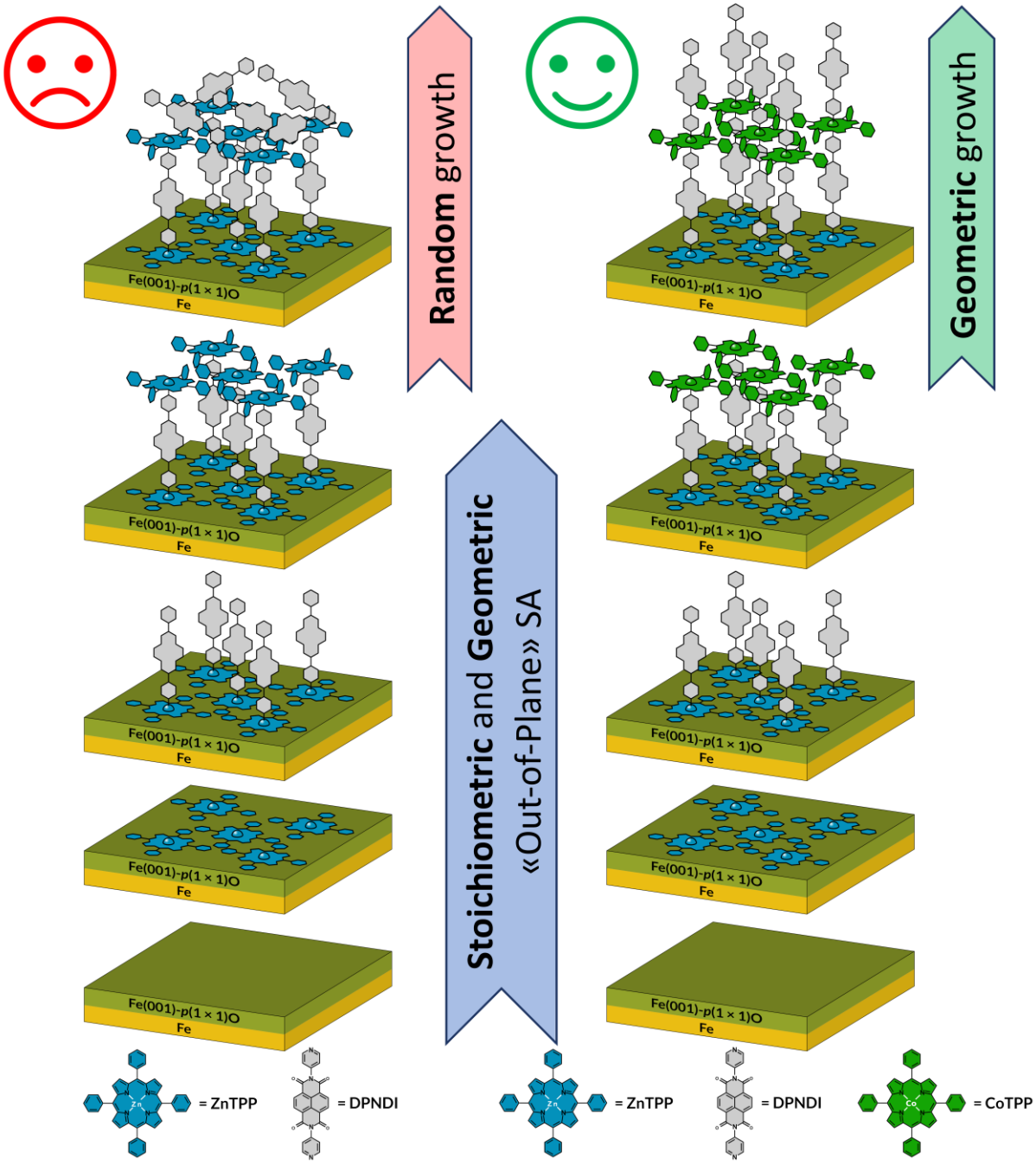


**Figure S2.** Full scheme of the 3D "out-of-plane" construction described in the manuscript. Left panel, construction based on ZnTPP/DPNDI SA system; right panel, construction based on ZnTPP/DPNDI/CoTPP SA system.

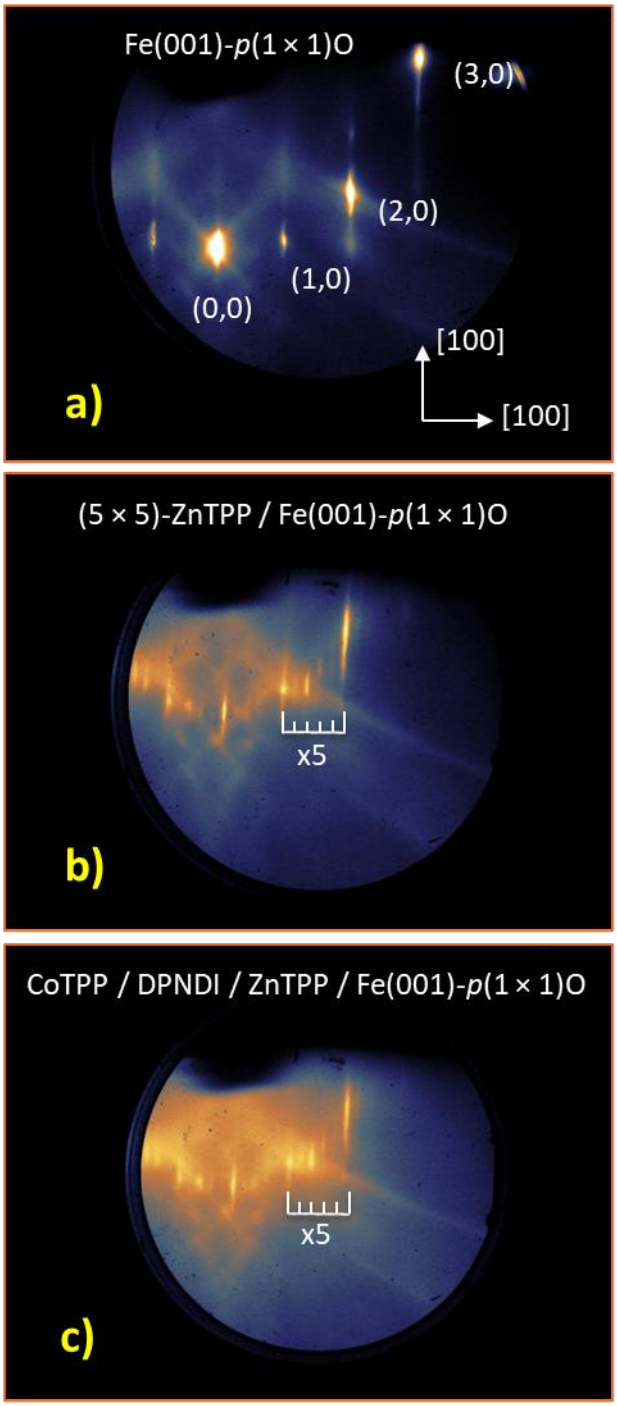


**Figure S3**. RHEED patterns at 15 kV: (a) diffraction pattern of the Fe(001)-*p*(1 × 1)O passivated surface; the brightest spot is the specularly reflected one, while the Bragg's peaks of integer order along the [100] direction are distributed on an arc of circumference; (b) pattern taken just after deposition of about 1 ML ZnTPP at RT on the same surface of the previous pattern; fractional spots of the 5th order can be appreciated in between the Bragg's peaks; (c) the five-fold diffraction spots are well visible on a 3-layer film of CoTPP/DPNDI/ ZnTPP/FeO; no extra spots are detectable, apart from an overall increase of the diffuse scattering background; the film is grown on the same substrate of previous pattern; the ZnTPP film was first annealed to 200˚C to improve ordering and desorb eventual 2nd layer molecules; a calibrated coverage of 1 ML DPNDI was then deposited at RT, followed by deposition of 1 ML CoTPP at RT.

[1] T. Schiros, G. Kladnik, D. Prezzi, A. Ferretti, G. Olivieri, A. Cossaro, L. Floreano, A. Verdini, C. Schenck, M. Cox, A. A. Gorodetsky, K. Plunkett, D. Delongchamp, C. Nuckolls, A. Morgante, D. Cvetko, I. Kymissis, Donor–Acceptor Shape Matching Drives Performance in Photovoltaics, *Adv. Energy Mater.* 3 (**2013**) 894–902.